CONF-860421--52

A MECHANISM OF SWELLING SUPPRESSION IN PHOSPHOROUS-MODIFIED Fe-Ni-Cr ALLOYS*

CONF-860421--52

DE86 011782

E. H. Lee and L. K. Mansur
Metals and Ceramics Division
Oak Ridge National Laboratory
Oak Ridge, TN 37831 (USA)

ABSTRACT

Five simple alloys were ion irradiated at 948 K in an experiment designed to investigate the mechanism of swelling suppression associated with phosphorous additions. One of the alloys was the simple ternary Fe-15Ni-13Cr, another had 0.05% P added and the other three had further additions of the phosphide precipitate-forming elements Ti and/or Si. Ion irradiations were carried out with heavy ions only (Ni or Fe) or with heavy ions followed by dual heavy ions and helium. The ternary with and without P swelled readily early in dose with or without helium. The other three alloys only showed swelling in the presence of helium and exhibited a long delay in dose prior to the onset of swelling. These displayed fine distributions of Fe_2P type phosphide precipitates enhanced by irradiation. The phosphide particles gave rise to very high concentrations of stable helium filled cavities at the precipitate matrix interfaces. The results were analyzed in terms of the theory of cavity swelling. The accumulation of the critical number of gas atoms in an individual cavity is required in the theory for point defect driven swelling to begin. It is concluded that the primary mechanism leading to swelling suppression is therefore the dilution of injected helium over a very large number of cavities. It is suggested that this mechanism may offer a key for alloy design for swelling resistance in high helium environments.

*Research sponsored by the Division of Materials Sciences, U.S. Department of Energy, under contract DE-AC05-84OR21400 with Martin Marietta Energy Systems, Inc.

1. INTRODUCTION

It has been observed that phosphorous-modified stainless steels exhibit resistance to cavity swelling during irradiation [1]. The remarkably high degree of swelling suppression associated with phosphorous additions renders such alloys among the most swelling resistant structural alloys available. In our previous work it was shown that a fine dispersion of phosphide precipitates develops in these alloys. The interfaces of these precipitates are occupied by a very high concentration of stable gas filled cavities. It was suggested that by distributing or diluting the helium in these alloys among this large number of cavities, the accumulation of the critical number of gas atoms in a cavity required for rapid point defect driven swelling was inhibited.

The critical number of gas atoms is that which theory dictates must be contained within a cavity in order for rapid point defect driven (as contrasted with gas driven) growth to begin [2–6]. It has a one-to-one correspondence with a related quantity, the minimum critical radius, which can be measured using transmission electron microscopy. The critical quantities arise as a result of competition between cavity growth by radiation induced point defect fluxes and cavity shrinkage by thermal vacancy emission. In general if a cavity is above the critical radius, then the thermal emission term is low enough for the radiation induced fluxes to dominate. However, the critical radius is reduced by the contained gas pressure. With n_g gas atoms a cavity will reside at a stable radius

$r_c^s(n_g)$, and the corresponding (larger) critical radius that must be reached for point defect driven growth is $r_c(n_g)$. As more gas is added to the cavity its stable radius is increased while its critical radius is decreased. When the critical number of gas atoms n_g^* is reached, r_c^s and r_c^c coincide at r_c^*, the minimum critical radius. When more gas is added, the critical radius vanishes, and a cavity of any radius containing more than n_g^* gas atoms will grow inexorably.

The existence of critical quantities leads to the expectation of bimodal cavity size distributions. When some of the cavities have accumulated more than n_g^* gas atoms, their growth to large sizes will be rapid, while their counterparts containing less than n_g^* gas atoms remain behind at their corresponding stable radius r_c^s. There will generally be a gap in size between the two populations. Thus, for example, even in phosphorous modified alloys it is expected that accelerated swelling will eventually begin when enough transmutation-produced or deliberately injected gas is accumulated; a bimodal cavity size distribution then should be observed.

The purpose of the present work is to examine in detail our hypothesis relating helium dilution at precipitate matrix interfaces to swelling resistance. A systematic series of experiments is carried out on a set of simple phosphorous-modified alloys. Observations of precipitates, interfacial cavities and bimodal size distributions are emphasized.

2. EXPERIMENTAL

Five simple alloys of increasing alloying content were employed: one is the base Fe-13Cr-15Ni alloy and four others are phosphorous modified

variants. In three of these, other alloying elements (Si,Ti) also were introduced in order to bring out increasing densities of phosphide precipitates. Table 1 gives the chemical compositions of the alloys.

Two types of ion irradiations were carried out on these alloys. In the first, Ni ions only were used. Thus the microstructural development in the absence of helium was determined. The second type of experiment consisted of a sequenced irradiation. First, Fe ions only were applied. This treatment induced a high density of phosphide precipitates in the phosphorous-bearing alloys and was intended to maximize the precipitate-matrix interfacial area in order to subsequently determine the extent of swelling suppression possible with helium dilution at interfaces. This step was followed by a simultaneous irradiation with both Fe and He ions to induce further microstructural evolution including cavities. (The use of either Fe or Ni ions has been shown to lead to equivalent results, both being self-ions of the alloys introduced in concentrations <1%.)

Solution annealed (1373 K/15 min) specimen disks 3 mm in diameter by 0.35 mm in thickness were irradiated at 948 K in the ORNL 5 MV/400 kV dual ion Van de Graaff accelerator system. The ion energies were 4 MeV for Fe and Ni and were sinusoidally ramped between 200 and 400 keV for the helium in order to spread it uniformly throughout the heavy ion damage region. After ion bombardment the specimens were electrochemically sectioned to a depth of 0.6 micrometer from the bombarded side and thinned from the back side to perforation. Microstructural examinations and analyses of precipitate compositions were carried out on a JEM 120 CX transmission electron

microscope with energy dispersive x-ray spectrometer. Details of both the bombardment facility and analyses procedures have been given elsewhere [7,8]. The procedures for data analysis were carried out in accordance with the guidelines described in ASTM Standards E521 and E942.

3. RESULTS

3.1 Irradiation Without Helium

In the phosphorous modified alloys, needle shaped phosphide precipitates nucleated early in dose at dislocation loops and line dislocations. Figure 1 shows the microstructures of all the alloys at 1 dpa. In a separate thermal aging experiment on the same alloys, it was found that phosphide formation was extremely sluggish, only giving rise to less than one one-thousandth the density of particles for an aging time of 1 yr at the bombardment temperature. Phosphide precipitates were formed at 1 dpa in all alloys containing phosphorous. However, at higher doses phosphides appear at much higher densities in the alloys containing silicon or titanium or both, as shown in Fig. 2. Titanium is the strongest phosphide former. The particle concentrations were greater than 6×10^{20} m^{-3} in alloys B11 and B12 containing titanium, about three times higher than that of alloy B10 with Si but no Ti, and about two orders of magnitude higher than that of alloy B9 with neither Si nor Ti. Table 2 gives the complete results of microstructural examination. Energy dispersive x-ray analyses of the particles revealed that they are typically $M_2(P,Si)$ having the Fe_2P

type hexagonal structure with lattice parameters a = 0.604 and c = 0.36 nm. In the alloys containing silicon and titanium, the precipitates contain about 10% Si and/or 10% Ti.

At high dose, two of the alloys, B1 and B9, showed significant swelling, while the alloys B10, B11, and B12 did not show any sign of cavities. The correlation of swelling suppression with the presence of the high density of phosphides is striking, as shown in Fig. 2. Phosphorous addition alone, when phosphide precipitates were very sparse, did not play any role in suppressing swelling as can be seen by comparing alloys B1 (no P) and B9 (with P) in Fig. 2. Cavity volume fractions in these two alloys reached about 4.6% in alloy B1 at 95 dpa and 3.5% in alloy B9 at 86 dpa.

The dislocation densities in all alloys at high doses were similar, about 2×10^{14} m^{-2}. Other precipitates also formed at much lower densities, mainly TiC and G-phase.

3.2 Sequenced Single and Dual Irradiations

Table 2 summarizes the ion doses in the first stage as well as the ion doses and helium injection levels in the second stage of these experiments together with the cavity and precipitate statistics. In these irradiations the precipitate densities observed were quite similar to those of the irradiations with no helium, about 2×10^{20} m^{-3} in alloy B10 and about 6×10^{20} m^{-3} in alloys B11 and B12. However, one specimen in each of B11 and B12 showed a factor of about five higher phosphide precipitate density.

Greater than 90% of the bubbles in these alloys were at phosphide-matrix interfaces, as expected (Fig. 3). No large cavities were observed at the lowest doses (~1 dpa) during the dual ion step even with the simultaneous injection of 95 appm He. At higher doses, 40 dpa in the most swelling resistant alloy B12, some of these bubbles had grown into large cavities leading to non-negligible swelling. At this stage a bimodal cavity size distribution was observed. Figure 3 illustrates the microstructure of alloy B12 observed in TEM. The largest diameter among the cavities in the smaller size class, corresponding to the minimum critical radius of the theory, was observed to be 2.5 nm and was the same for each of the alloys B10, B11 and B12. The micrograph of alloy B12 shown in Fig. 3 also shows the small stable helium filled cavities, accompanied by fewer much larger growing cavities. The stable cavity densities are generally an order of magnitude higher than the phosphide precipitate particle densities.

In the alloys containing titanium, B11 and B12, a high density of small TiC particles formed. The precipitates were not uniformly distributed; in some areas their concentrations were as much as 4–5 times the density of the phosphide particles. In areas where TiC was plentiful, the phosphide phase was suppressed because both phases compete for titanium. However, since these small TiC particles generally appear to be associated with only one helium bubble, the phosphides provide a much stronger diluent for helium. In addition, particles of silicon rich G-phase were formed in

alloy B12 at high dose. An example is shown at 81 dpa in Fig. 3, where the large objects are G-phase particles. Many small bubbles were also found at the G-phase/matrix interface. In addition, many of the G-phase particles were associated with large growing cavities. Because these particles are large and relatively few in number, they offer negligible dilution of helium by the formation of interfacial bubbles. On the other hand their individually large size appears to be quite effective at accelerating the growth stage of cavities attached to them that have exceeded the critical radius. This rapid growth of cavities attached to large G-phase precipitates is seen as a manifestation of the precipitate point defect collection mechanism described by Mansur [9] and Lee et al. previously [10].

Special cases of the sequential irradiations summarized in Table 2 are those indicated with a zero in the second column. These did not receive a heavy-ion-only dose prior to simultaneous irradiation with heavy-ions and helium ions. These irradiations resulted in precipitation essentially similar to that of the sequential irradiations. In alloys B10, B11 and B12 no appreciable cavity formation was observed. This absence of cavities is attributed to the much lower levels of helium accumulated in these specimens, compared with those subjected to sequential irradiations where cavities were observed (30 appm compared with 74 to 440 appm). On the other hand in alloys B1 and B9 (results not shown in Table 2), the simultaneous injection of helium did not significantly alter the swelling compared to the no-helium case.

4. ANALYSIS

To aid in the interpretation of these results, calculations of the expected minimum critical cavity radius, r_c^*, and critical number of gas atoms, n_g^*, have been performed. The general forms of the expressions given by Mansur et al. [11] are used in the present analysis,

$$r_c^* = \frac{2\gamma}{f}\left(\frac{1+\delta}{2+\delta}\right) \tag{1}$$

$$\text{where } f = \frac{kT}{\Omega} \ell n\, S \tag{2}$$

and

$$S = \frac{Z_v^c D_v C_v - Z_i^c D_i C_i}{Z_v^c D_v C_v^e} \tag{3}$$

The corresponding expression for the critical number of gas atoms is

$$n_g^* = \frac{32\,\pi\gamma^3}{f^2 kT}\,\frac{(1+\delta)^2}{(2+\delta)^4} \tag{4}$$

Here, $\delta = (1 + 3\beta)^{1/2}$, where $\beta = Bf/kT$ with B denoting the Van der Waals volume exclusion correction. The symbol γ denotes surface energy, Ω denotes atomic volume, D denotes diffusion coefficient, C denotes physical point defect concentration and Z^c denotes the capture efficiency

of a cavity for point defects. These symbols are specialized by the subscripts v and i, denoting vacancies and interstitials, respectively. The symbol C_v^e denotes thermal equilibrium bulk vacancy concentration and kT has its usual meaning. Full expressions for the point defect concentrations and other quantities dependent on materials parameters and irradiation conditions are given in Ref. [5].

Thus the achievement of the critical quantities depends on a number of system parameters that are both implicit and explicit in the above equations. Three parameters are of primary interest here: the point defect sink densities, the surface free energy, and the precipitate matrix interfacial area through its effect on the number of stable cavities.

Dislocation, cavity, and precipitate sink strengths for point defects vary throughout the irradiations. However, typical results can be obtained from Table 2. The dislocation densities were about 2×10^{14} m^{-2}. The total (stable and growing) cavity density was typically about 2×10^{20} m^{-3} for alloys B1 and B9, 6×10^{21} m^{-3} for alloy B10 and 2×10^{22} m^{-3} for alloys B11 and B12. These values are used as a component of the sink strengths necessary to calculate the theoretically predicted value of the critical radius for each alloy. The size of the small cavities is also a necessary input for the sink strength calculations. Since the average stable cavity size increases with the amount of helium injected (because of the increasing sink strength) as shown in Fig. 3, one-half the observed stable cavity size near the onset of bias driven swelling is used in the sink strength determination. Since no stable cavities are observed in alloys B1 and B9, sink strengths for these had to be assumed corresponding

to radii below the resolution limit of electron microscopy (0.5 nm). However, the calculated value of r_c^* is independent of this sink strength since dislocations are the dominant sink in these alloys. Other important parameters are the surface free energy, here taken as the approximate center of the range (2 J/m^2) of both experimental and theoretical values for iron, chromium, and nickel [12], the vacancy migration and formation energies (1.2 and 1.6 eV, respectively) and the effective bias (1.5%), where its low value also accounts for the fact that the defect production rate is generally less than the displacement rate used in the present calculations.

The calculated values of r_c^* and n_g^* as well as the measured values of r_c^* are shown in Table 3. The experimental and calculated values agree well except in alloys B1 and B9. However, when the surface energy for these alloys is reduced from 2 to 1 J/m^2, good agreement is obtained. The critical radius is reduced by a factor of 2 by this change in accordance with Eq. (1). We believe this lower value of surface energy may be reasonable in view of the high concentration of impurity oxygen in alloys B1 and B9, as shown in Table 1. Oxygen is well known to be a surface active element that lowers the surface free energy by as much as 50% with less than 25% of a monolayer coverage [13,14]. Recently, Zinkle et al. [15] reported that cavity formation in copper was triggered by less than 40 appm oxygen, and their interpretation was that it essentially lowered the surface free energy. Similarly, our recent work [16] has shown that less than 30 appm oxygen stabilized cavity formation in Fe-Ni-Cr alloys. This oxygen was

accelerator injected, however, and it appears to be much more effective than oxygen introduced during normal fabrication. Nevertheless, the very high levels (1000 appm) in alloys B1 and B9 may well have been sufficient to modify the surface energy.

The presence of more cavities in response to the increased interfacial area provided by phosphide precipitates has another yet stronger effect than the simple increase in point defect sink strengths and consequent increase in r_c^* and n_g^*. The increased number of cavities dilutes helium atoms among more sites, delaying the buildup of n_g^* gas atoms in any cavity, and thus delaying the onset of bias driven swelling. The predicted effect is dramatic as can be seen in the last column of Table 3. In alloys B1 and B9, the amount of helium estimated to be required for rapid swelling is only 0.8 appm, while that in the phosphide forming alloys is almost 200 times larger.

5. DISCUSSION

It follows from the analysis above that three related reasons reinforce each other to cause the simple ternary alloy to begin swelling very early in dose. The first is that there is no gas dilution by profuse bubble formation at precipitate matrix interfaces. Only a relatively small number of cavities are available to accommodate gases. Second is the fact that the critical radius and the critical number of gas atoms are also smaller than those required in the alloys containing precipitate forming (and oxygen gettering) elements Si and Ti. This lower critical radius is attributed mainly to the presence of high levels of oxygen in this alloy,

which reduces the surface free energy of the cavities to the point where the critical radius is below the observation limit. Another reason for the reduced critical radius is that the point defect sink strength in this alloy is very low compared to the alloys with precipitates, and a low sink strength is associated with a small critical radius [17]. With such a small critical radius required for point defect driven swelling, there is apparently enough residual gas in the alloy to supply the correspondingly very small critical number of gas atoms to trigger swelling; thus the observation that the alloy swells even without helium injection.

All of the statements above also apply to the ternary modified with phosphorous only. The addition of phosphorous alone does not provide any significant reduction in swelling, nor does it induce any significant precipitation of phosphide particles. Thus the three attributes described above are not mitigated with the addition of phosphorous alone to the ternary.

When the phosphide forming and oxygen gettering elements Si and Ti are also introduced, then significant swelling suppression occurs. Based on the calculations described, the main reason for swelling suppression is the helium dilution effect of the profuse formation of bubbles on precipitate-matrix interfaces. Secondary effects are (1) the increase in the critical number of gas atoms required for point defect driven cavity growth by the removal of the surface active oxygen,* (2) the increase in the critical

*Eqs. (1) and (4) show that n_g^* is proportional to $r_c^*\gamma$ and that r_c^* is proportional to γ, so that doubling γ increases n_g^* by a factor of eight.

number caused by an increase in overall point defect sink strength, and (3) the removal of the excess oxygen the possibility of residual gas triggering swelling is eliminated.

It also follows from the analyses that any swelling resistant alloy designed on the principle of helium dilution should eventually swell at high dose. The question arises as to how long swelling can be delayed in a practically achievable alloy.

In the phosphide containing alloys described herein, significant swelling has been delayed to the range of 50–100 dpa and a few hundred appm He. However, these are extremely simple solution annealed materials that were designed to investigate systematically the swelling suppressing mechanism of helium dilution. In very recent experiments on more complex and highly cold worked alloys, swelling has been suppressed to well over 100 dpa and well over 1000 appm He [18]. In these cases an even higher concentration of phosphide precipitates was nucleated on the cold work dislocations, so that the number of bubbles available for helium dilution was increased significantly. At the same time the critical radius was increased by yet another factor of two because of the further increase in point defect sink strength provided by the dislocations, cavities, and precipitates. These alloys are among the most swelling resistant alloys available.

Other hypotheses have also been put forward to explain the swelling resistance of phosphorous modified alloys. One is that the phosphide precipitates may have provided enough extra point defect sink strength to

sufficiently lower the point defect concentrations and the swelling rate of growing cavities [19]. However, a recent analysis by Brailsford and Mansur [20] showed that this could not account for all of the swelling suppression reported by Lee et al. [1] in a high phosphorous alloy. Another suggestion is that the phosphorous atom increases point defect diffusion rates, thus lowering point defect concentrations and in turn lowering cavity nucleation [21]. The present results, however, are not consistent with this idea. The alloy with phosphorous additions alone swells as readily as the pure ternary. In the three alloys with phosphide precipitates there is no difficulty in nucleating cavities (Table 2). The cavities simply do not grow readily until they accumulate the critical number of gas atoms.

6. SUMMARY

A series of simple phosphorous-modified alloys was prepared to investigate the mechanism of swelling suppression in phosphorous-containing alloys. One of the alloys was a simple ternary Fe-15Ni-13Cr, another had 0.05% P added, while three others had the same amount of P together with additions of Ti and/or Si. Ion irradiations were carried out, using either heavy ions only with no helium added or in sequenced fashion first with heavy ions only and next with dual heavy-ions and helium.

In the ternary and the ternary plus P alloys, early and large swelling occurred. In the other alloys swelling was suppressed, most significantly for the alloy containing both Si and Ti. The suppression of swelling was correlated with the appearance of a high density of Fe_2P type phosphide

precipitates, which were only prevalent in the alloys containing Si and/or Ti. On these precipitates there was profuse formation of helium bubbles.

These results confirmed the hypothesis that these experiments were designed to investigate. The swelling suppression effect of phosphorous takes place by a mechanism of helium dilution. With the very high density of cavities achieved by the introduction of precipitate-matrix interfaces as helium traps, the time to accumulate the critical number of gas atoms in a cavity is extended. The critical number of gas atoms is a concept arising in the theory of swelling, being that number required before rapid swelling driven by point defect absorption can begin. Bimodal cavity size distributions were observed when swelling began, consistent with the hypothesized mechanism. The largest size in the smaller group of cavities is taken as the critical radius corresponding to the critical number of gas atoms. Quantitative calculations reproduce the measured critical size and confirm that the swelling suppression is a result of the delay in accumulating the critical number of gas atoms by precipitate-based helium dilution.

It is suggested that these results may furnish a simple physical basis for the design of swelling resistant alloys in the high helium environment of fusion reactors.

REFERENCES

1. E. H. Lee, L. K. Mansur, and A. F. Rowcliffe, J. Nucl. Mater. 122&123 (1984) 299.
2. K. C. Russell, Acta Met. 26 (1978) 1615.
3. J. A. Spitznagel, W. J. Choyke, N. J. Doyle, R. B. Irwin, J. R. Townsend, and J. N. McGruer, J. Nucl. Mater. 108–109 (1982) 537.
4. R. Stoller and G. R. Odette, "Effects of Radiation on Materials" Eleventh Conf., ASTM 782, eds. H. R. Brager and J. S. Perrin (Amer. Soc. for Testing and Materials, 1982) p. 275.
5. L. K. Mansur and W. A. Coghlan, J. Nucl. Mater. 119 (1983) 1.
6. R. Bullough and S. M. Murphy, J. Nucl. Mater. 133&134 (1985) 92.
7. M. B. Lewis, N. H. Packan, G. F. Wells, and R. A. Buhl, Nucl. Instr. and Meth. 167 (1979) 223.
8. E. H. Lee, P. J. Maziasz, and A. F. Rowcliffe, Conf. on Phase Stability During Irradiation, Pittsburgh, PA, eds., J. R. Holland, L. K. Mansur, and D. I. Potter, TMS-AIME (Oct. 1980) 191.
9. L. K. Mansur, Phil. Mag. 44A (1981) 867.
10. E. H. Lee, A. F. Rowcliffe and L. K. Mansur, J. Nucl. Mater. 103&104 (1981) 1475.
11. L. K. Mansur, E. H. Lee, and P. J. Maziasz, this conference.
12. L. E. Murr, Interfacial Phenomena in Metals and Alloys, Addison-Wesley Pub. Co. (1975) 185.
13. M. McLean and E. D. Hondros, J. Mater. Sci. 8 (1973) 349.
14. E. D. Hondros, Acta Met., Vol. 16, (1968) 1377.

15. S. Zinkle, W. G. Wolfer, G. L. Kulcinski, and L. E. Seitzman, submitted to Phil. Mag.

16. E. H. Lee and L. K. Mansur, to be published.

17. W. A. Coghlan and L. K. Mansur, in Effects of Radiation on Materials: 12th Inter. Symp., ASTM 870, F. A. Garner and J. S. Perrin, eds., American Society for Testing and Materials, Philadelphia, 1985, p. 481.

18. E. H. Lee and L. K. Mansur, to be published.

19. L. K. Mansur, M. R. Hayns, and E. H. Lee, Conf.on Phase Stability During Irradiation, Pittsburgh, PA, eds., J. R. Holland, L. K. Mansur, and D. I. Potter, TMS-AIME (Oct. 1980) 359.

20. A. D. Brailsford and L. K. Mansur, J. Nucl. Mater. 103&104 (1981) 1403.

21. F. A. Garner and H. R. Brager, J. Nucl. Mater. 133&134 (1985) 511.

FIGURE CAPTIONS

Fig. 1. TEM microstructures irradiated with 4 MeV Ni^{++} ions to 1 dpa at 948 K: (a) B1, (b) B9, (c) B10, (d) B11, and (e) B12 alloys.

Fig. 2. TEM microstructures (top) of alloys irradiated to 70 dpa with 4 MeV Ni^{++} ions at 948 K together with corresponding carbon extraction replicas (bottom) to show relative precipitate number densities and morphologies: (a) B1, (b) B9, (c) B10, (d) B11, and (e) B12 alloys.

Fig. 3. TEM microstructures of alloy B12 irradiated sequentially with 4 MeV Fe^{++} ions alone and then simultaneously with helium: (a) 23 dpa + (95 appm He/1 dpa), (b) 40 dpa + (180 appm He/40 dpa), and (c) 34 dpa + (319 appm He/81 dpa).

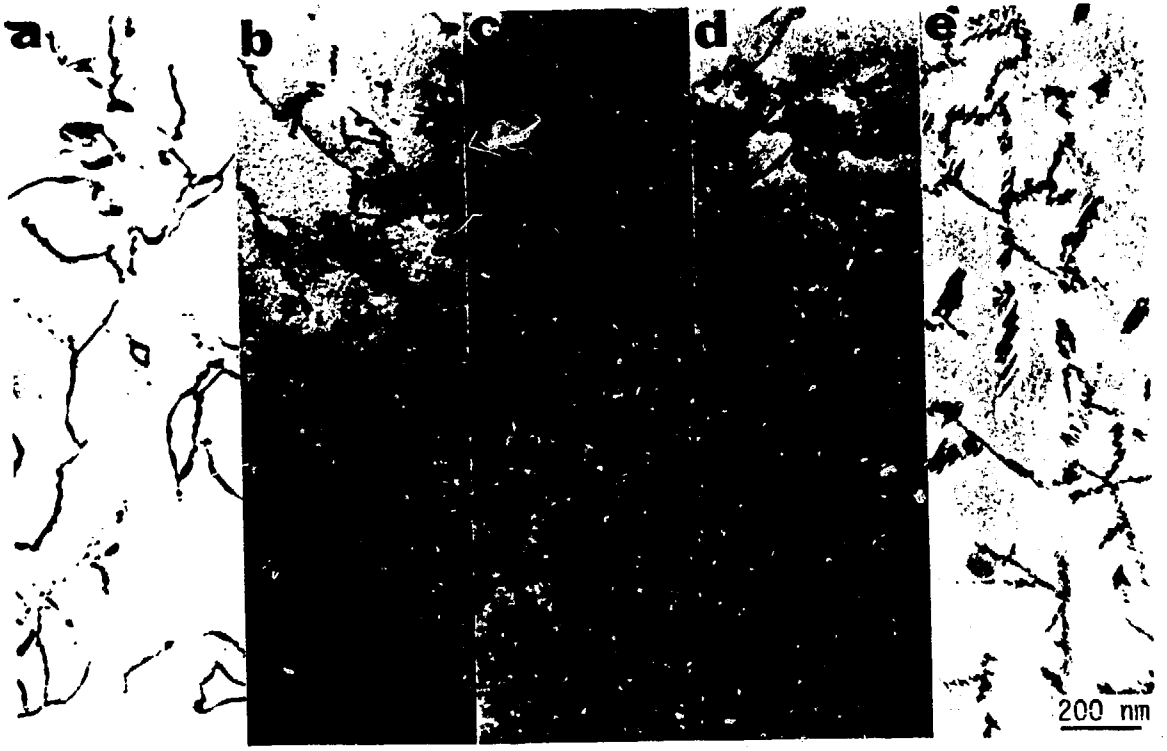

F:9.1.

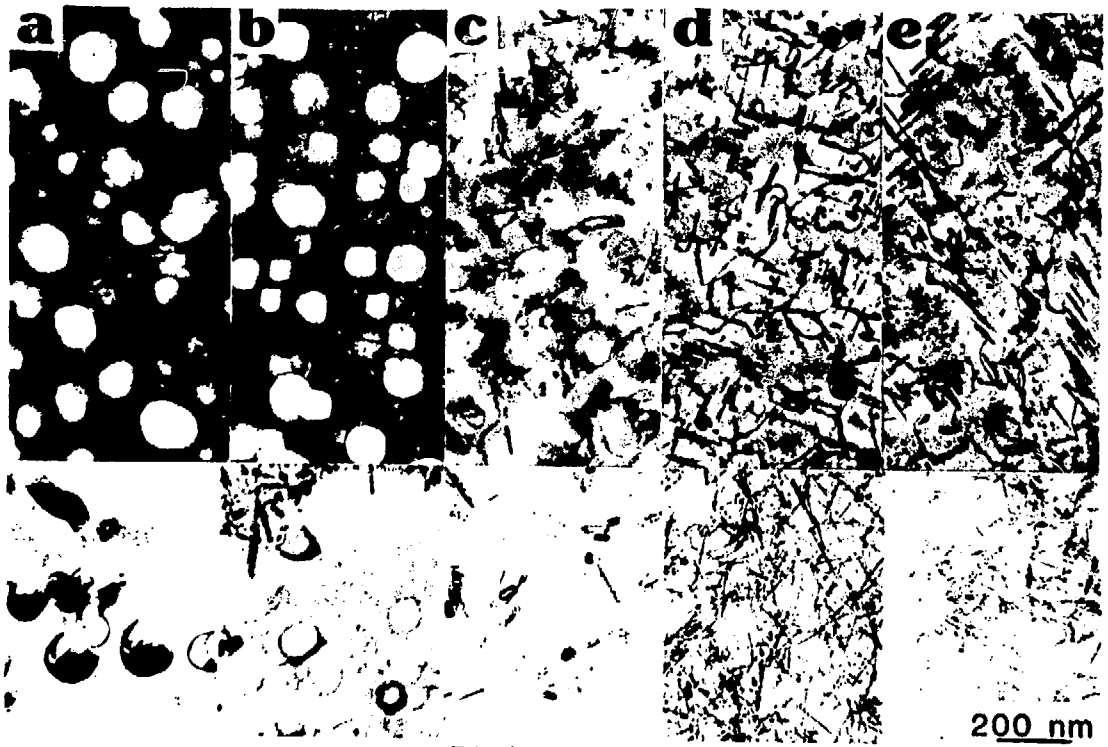

70 dpa/675 C

Fig 2

ORNL-PHOTO 1538-86

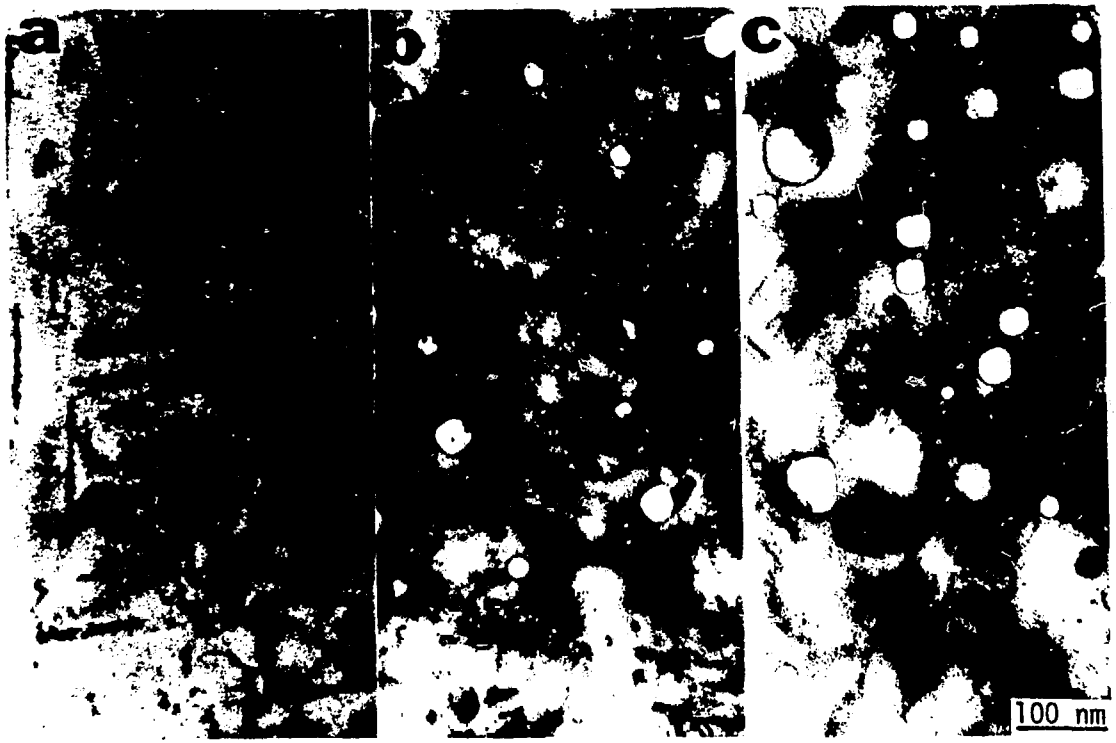

Fig. 3

TABLE 1—Chemical Composition of Alloys in Weight Percent

Alloys	Fe	Cr	Ni	Mo	Mn	Si	Ti	C	P	N	O (appm)
B1	Bal	13.79	14.95	--	--	--	--	--	--	0.010	0.030 (1050)
B9	Bal	13.71	15.23	--	--	--	--	--	0.049	0.009	0.031 (1050)
B10	Bal	13.64	15.15	--	--	0.84	--	--	0.050	0.009	0.020 (700)
B11	Bal	13.63	15.20	--	--	--	0.18	0.041	0.049	0.011	0.013 (455)
B12	Bal	13.58	15.15	--	--	0.83	0.17	0.044	0.049	0.010	0.004 (140)

Dashed lines: Not intentionally added, but trace amounts of these elements exist together with other impurity elements.

TABLE 2—Microstructural Data of Irradiated Alloys*

Alloys	Dose		Cavity concentration (m^{-3})	Average cavity diameter (nm)	Cavity volume fraction (%)	Bubble concentration (m^{-3})	M_2P concentration (m^{-3})
	Ion only (dpa)	He+Ions (appm/dpa)					
B1	95	0	2.2×10^{20}	63	4.6	--	--
B9	86	0	2.0×10^{20}	65	3.5	--	$<5 \times 10^{18}$
	85	0	--	--	--	--	$\sim 2 \times 10^{20}$
	0	30/78	--	--	--	--	$\sim 2 \times 10^{20}$
B10	25	74/9	3.3×10^{19}	52	<0.1	--	2.5×10^{20}
	30	95/18	2.2×10^{20}	21	0.2	--	2.2×10^{20}
	49	440/60	4.2×10^{20}	34	1.3	5.9×10^{21}	--
	97	0	--	--	--	--	$\sim 6 \times 10^{20}$
	0	30/85	--	--	--	--	$\sim 6 \times 10^{20}$
B11	35	95/1.2	--	--	--	1.2×10^{22}	6.5×10^{20}
	43	74/24	1.2×10^{21}	19	0.4	1.8×10^{22}	3.2×10^{21}
	42	319/90	2.1×10^{21}	31	3.1	1.2×10^{22}	--
	59	0	--	--	--	--	$\sim 6 \times 10^{20}$
	0	30/61	--	--	--	--	$\sim 6 \times 10^{20}$
B12	23	95/1	--	--	--	2.8×10^{22}	2.8×10^{21}
	40	180/40	3.9×10^{20}	24	0.4	2.2×10^{22}	6.0×10^{20}
	34	319/81	3.3×10^{20}	30	0.7	$>2 \times 10^{21}$	6.4×10^{20}

*Dislocation densities were typically $\sim 2 \times 10^{14}$ m^{-2} for all alloys.

Dashed lines: Not measurable.

TABLE 3—Calculations of r_c^*

Alloys	Dislocation density (m^{-2})	Cavity density, N_c (m^{-3})	Surface energy (J/m^2)	Experimental r_c^* (nm)	Calculated r_c^* (nm)	Calculated N_g^* (no.)	He conc.† $N_g^* \times N_c$ (appm)
B1	2×10^{14}	2×10^{20}	2.0	<0.5?	0.96	393	0.8
			1.0		0.48	49	
B9	2×10^{14}	2×10^{20}	2.0	<0.5?	0.96	393	0.8
			1.0		0.48	49	
B10	2×10^{14}	6×10^{21}	2.0	1.25	1.05	475	43
B11	2×10^{14}	2×10^{22}	2.0	1.25	1.27	688	142
B12	2×10^{14}	2×10^{22}	2.0	1.25	1.27	688	142
CW A7	2×10^{15}	1×10^{23}	2.0	2.5	1.77	1342	1384

†Helium concentration needed to reach critical size.